World Academy of Science, Engineering and Technology
International Journal of Civil and Environmental Engineering
Vol:12, No:6, 2018

Assessing Overall Thermal Conductance Value of Low-Rise Residential Home Exterior Above-Grade Walls Using Infrared Thermography Methods

Matthew D. Baffa

***Abstract*—**Infrared thermography is a non-destructive test method used to estimate surface temperatures based on the amount of electromagnetic energy radiated by building envelope components. These surface temperatures are indicators of various qualitative building envelope deficiencies such as locations and extent of heat loss, thermal bridging, damaged or missing thermal insulation, air leakage, and moisture presence in roof, floor, and wall assemblies. Although infrared thermography is commonly used for qualitative deficiency detection in buildings, this study assesses its use as a quantitative method to estimate the overall thermal conductance value (U-value) of the exterior above-grade walls of a study home. The overall U-value of exterior above-grade walls in a home provides useful insight into the energy consumption and thermal comfort of a home. Three methodologies from the literature were employed to estimate the overall U-value by equating conductive heat loss through the exterior above-grade walls to the sum of convective and radiant heat losses of the walls. Outdoor infrared thermography field measurements of the exterior above-grade wall surface and reflective temperatures and emissivity values for various components of the exterior above-grade wall assemblies were carried out during winter months at the study home using a basic thermal imager device. The overall U-values estimated from each methodology from the literature using the recorded field measurements were compared to the nominal exterior above-grade wall overall U-value calculated from materials and dimensions detailed in architectural drawings of the study home. The nominal overall U-value was validated through calendarization and weather normalization of utility bills for the study home as well as various estimated heat loss quantities from a HOT2000 computer model of the study home and other methods. Under ideal environmental conditions, the estimated overall U-values deviated from the nominal overall U-value between ±2% to ±33%. This study suggests infrared thermography can estimate the overall U-value of exterior above-grade walls in low-rise residential homes with a fair amount of accuracy.

***Keywords*—**Emissivity, heat loss, infrared thermography, thermal conductance.

I. Introduction

INFRARED (IR) thermography is a non-destructive test method used to estimate surface temperatures of objects [1]. It has been used over the past few decades for the purposes of building monitoring and diagnostics [2]. IR thermography is capable of identifying locations and extent of heat loss, damaged or missing thermal insulation, air leakage, moisture, and thermal bridging in building envelopes [3]. IR thermography is based on Planck's law, which states that all bodies radiate energy as electromagnetic waves travelling at the speed of light at temperatures greater than absolute zero. Given the typical temperatures experienced within building envelopes, wavelengths of radiated energy are within the IR range of the electromagnetic spectrum between 2 µm to 5.6 µm and 8 µm to 14 µm spectral bands [2]. These wavelengths radiated from building envelopes are not visible to the human eye. Thermal power per area (W/m^2) emitted by objects is calculated through the Stefan-Boltzmann Law [3]:

$$Q = \sigma \varepsilon T^4 \quad (1)$$

where σ is the Stefan-Boltzmann constant (5.67×10^{-8} $W/m^2 \cdot K^4$), ε is the emissivity of the object, and T is the absolute surface temperature of the object (K).

IR thermal imagers are the devices that capture the amount of IR energy radiated from objects and convert it into a temperature profile image, providing that the correct emissivity of the target object is known. The temperature profile image contains different colours corresponding to a range of temperatures measured from target objects. Typically, brighter and darker colours are associated with warmer and colder temperature readings, respectively. The measurement accuracy of IR thermal imagers is influenced by several different factors including but not limited to the emissivity of the object, air temperature, wind speed, atmospheric particles and distance and angle between the thermal imager and target object [4].

The emissivity of an object is the fraction of energy that it radiates compared to a blackbody, or perfect emitter with an emissivity of 1, at the same surface temperature. Emissivity values range between 0 and 1 with common building materials having emissivity values greater than 0.8. The emissivity of an object is dependent on wavelength within the IR range, temperature, surface condition [2] and microstructure [5]. Emissivity is dependent on wavelength as objects absorb and emit energy at different wavelengths. Reference [2] conducted a study on the emissivity of plaster and stone materials at varying surrounding air temperatures ranging from 0 °C to 100 °C. They found that, in the 3 µm to 5.4 µm electromagnetic (mid) wavelength range, emissivity increased with an increase in air temperature, whereas in the 8 µm to 12 µm (long) electromagnetic wavelength range, emissivity decreased with an increase in air temperature. These changes

M. D. Baffa is a graduate of the Bachelor of Applied Science (BASc) and the Master of Engineering (MEng) Civil Engineering programs at the University of Toronto. He is now a Project Manager and Engineering Intern (EIT) at Building Sciences Inc. in Concord, Ontario (e-mail: matthew@buildingsciencesinc.com).

in emissivity with different air temperatures for a given wavelength range likely occurred as mid wavelength emissions from objects are sensitive to high temperatures such as 100 °C, whereas long wavelength emissions from objects are sensitive to low temperatures such as 0 °C [6]. Objects with darker surface colours have higher emissivity values [2]. Objects with smooth surfaces such as metals have low emissivity values due to their electron structure. Object microstructure affects its porosity moisture content, which can change its surface texture and colour [5]. Air temperature can affect the functionality of the thermal imaging device, allowing for inaccurate readings due to drifting effects. However, thermal imaging devices have internal compensation systems to correct for any temperature effects. Air temperature also affects the surface temperature of target objects, which is related to the amount of energy radiated to thermal imaging devices. Extreme air temperatures can result in less precise IR thermography measurements. The presence of wind influences surface temperatures of target objects by means of forced convective heat loss. It is recommended that IR thermography shall not be conducted outdoors during periods of wind except in the case of air leakage of a building being assessed through doors and windows. Atmospheric particles such as water vapour and carbon dioxide can attenuate radiation from target objects, causing thermal energy to be scattered. This attenuation creates two wavelength ranges; 3 μm to 5 μm and 8 μm to 12 μm. The 8 μm to 12 μm range is preferred in IR thermography as it has a greater sensitivity to air temperature and transmits well through smoke. Distance and angle between objects and thermal imagers affect the accuracy of data collection. Thermal imagers that measure farther away from target objects generate less accurate measurements as they are detecting radiation from a larger surface area, making each point on the thermal image an averaged value. Similarly, measurements taken at acute angles lose detail compared to orthogonal measurements [4]. Reference [7] suggested angles of thermal imagers towards target objects between 5 to 50° to avoid reflection of the thermal imager into the generated thermal images. Other factors include the different types of energy measured by thermal imagers. When measuring the energy radiated from target objects, temperature readings generated from thermal imagers also include thermal energy from surrounding objects that is reflected from the surface of the target object and thermal energy emitted from the atmosphere. It is suggested that atmospheric radiation can be neglected at short distances from the target object [8].

Reference [9] conducted a study on the evaluation of building materials using IR thermography. They found that emissivity, air temperature, relative humidity, reflective temperature, and colour influenced IR thermography measurements. They partially submerged two cellular concrete specimens in water and subjected them to identical drying periods followed by different ambient air temperatures and relative humidity in different climatic chambers. The thermal images were obtained using emissivity values of 0.62, 0.85, 0.91, and 0.95. The thermal images with an emissivity value of 0.62 differed from those obtained from the remaining emissivity values, which produced similar thermal images. Ambient air temperature and relative humidity in the climatic chambers influenced the presence of evaporative cooling of the specimen surfaces, which therefore affected their surface temperature measurements. Objects in thermal and hygroscopic equilibrium with surrounding air were not able to generate thermal images. The authors concluded that objects must vary at least 1 °C in temperature from ambient air in order for thermal images to be generated. Reflective thermal energy becomes important with low emissivity opaque objects, as low emissivity is equivalent to high reflectivity, allowing for large variations in surface temperature measurements [10]. The authors found that varying surface colours of different objects on a church exterior wall in Portugal influenced IR thermal images as darker colours emitted more thermal energy than brighter colours. Its effect was more prominent with larger temperature differences between the object surface and ambient air.

As a result of the factors influencing the measurements of thermal imagers, several environmental conditions are agreed upon in the literature to ensure proper execution of IR thermography. The minimum difference between the indoor and outdoor air temperature required to produce sufficient heat loss through building envelopes is 10 °C [3], [11], [12]. This air temperature difference can be achieved passively under normal building operation or actively using external heat sources [7]. Outdoor air temperature swings of less than 6 °C are recommended 12 hours prior to IR thermography measurements being carried out in order to achieve a steady state condition of heat flow [11]. Outdoor wind speeds should not exceed 5 m/s [4], [11]. Local wind speeds on the façade of the building should not exceed 0.5 m/s to minimize forced convective heat losses [11]. Measurements are best taken between 4:00 A.M. and 6:00 A.M. to avoid solar radiation on exterior walls, allow solar radiation stored in exterior walls from the previous day to dissipate and provide an optimal air temperature difference between the indoor and outdoor spaces [11]. Measurements are ideally conducted between the autumn and spring seasons for rapid dissipation of heat from solar radiation [1]. Reference [13] investigated the effect of solar radiation on exterior walls with varying amounts of cladding thermal mass. They found that exterior walls with larger amounts of thermal mass took longer to dissipate the heat absorbed from solar radiation. The cloud conditions should be overcast for 12 hours prior to IR thermography measurements being taken to reduce radiation heat losses to the sky. Measurements should not be taken on days of rain [11]. Moist surfaces retain absorbed heat longer than dry surfaces, causing objects to radiate heat at a later period of time [4]. Moisture in objects can cause surface cooling due to evaporation, thus altering surface temperature measurements [9]. Thermal conductivity of building materials increases in the presence of moisture [14]. Quasi-steady state conditions should be achieved 3 to 4 hours prior to IR thermography proceeding [3]. Heating systems must be operating during IR thermography testing to ensure sufficient air temperature

differences between the interior and exterior of buildings are present [1].

Reference [1] summarized the advantages of IR thermography as a non-destructive test method. The ease of use of thermal imagers in IR thermography generates results rapidly and requires minimal access to target objects. Additionally, the operations of building systems do not require stoppage during IR thermography testing. These advantages make the test method cost effective. Reference [7] mentioned advantages such as safety, ease of interpretation of results, and ability to detect deficiencies invisible to the human eye. Furthermore, they attributed the effectiveness of IR thermography to readily accessible and relatively low-priced thermal imaging devices that are used for inspections of building envelope deficiencies to reduce energy consumption in the building sector.

IR thermography is capable of detecting several deficiencies in building envelopes during energy audits by identifying locations of heat loss and heat gain. Thermal insulation prevents heat loss by conduction during heating seasons and prevents heat gain during cooling seasons, thus influencing exterior wall surface temperatures [4]. During the preferred autumn to spring months for testing, IR thermography detects warm spots on outer surfaces of exterior walls and cold spots on interior surfaces of exterior walls that correspond to missing, misplaced, damaged, or saturated thermal insulation [1]. Insulation deficiencies appear to have defined edges that trace its shape and location in thermal images. Air leakage through doors and windows in buildings occurs through infiltration (air entering) or exfiltration (air escaping). IR thermography measures the temperature of surfaces that air leaks through rather than the temperature of the leaking air. This temperature indicates whether infiltration or exfiltration is occurring. Moisture reduces the effectiveness of thermal insulation. Moist insulation in wall or roof assemblies of buildings appears adjacent to locations with warmer surface temperatures as heat is lost in comparison to sound areas that lose less heat. Moist insulation appears to have a patchy pattern in thermal images. Thermal bridging occurs when structural elements of buildings are placed through thermal insulation. These structural elements have lower thermal resistances than the surrounding thermal insulation, causing heat loss during winter or gain during summer months, thus influencing exterior wall surface temperatures [4].

IR thermography has primarily been used as a test method for qualitative analysis [15], [16]. Reference [1] suggested that IR thermography should only be used during energy audits to detect deficiencies in building envelopes due to unknown parameters such as air leakage through joints, windows and doors, and outdoor atmospheric conditions. Its use is not recommended in determining the thermal conductance values (U-values) of building envelope walls. The only standardized test method for the in-situ measurement of heat flow through exterior wall assemblies, which can determine the U-value of wall assemblies, is the heat flux meter (HFM) method in the ISO Standard 9869 [17], [18]. The HFM method has demonstrated in previous studies that the U-value of exterior wall assemblies is generally underestimated through calculations using standards such as ISO Standard 6946 [19] by 14% to 28% [12], [20], but can also vary between 50% below and 153% above the measured U-value from the HFM method [21]. The HFM method, however, requires a timeframe between 72 hours and one week for testing and acquiring data. Additionally, the HFM method only measures heat flow through points in a wall and does not provide accurate results when heat flow through non-homogeneous exterior wall types is required to be measured [12].

Reference [3] mentioned that the use of IR thermography as a quantitative method has been debated over the past few decades. They suggested that the use of IR thermography in determining U-values of building envelopes is particularly useful for energy performance classification of older buildings with very little construction information available. Their study investigated the use of IR thermography indoors to determine the overall U-value of the masonry walls, roofs, and glazing of five study homes in Cyprus. They estimated overall U-values that deviated 10% to 20% above the nominal overall U-values. Their sensitivity analysis indicated that the most influential parameters to the accuracy of estimated overall U-values were the difference between the wall surface and reflected temperatures and emissivity values of building components. Reference [15] conducted a similar study outdoors on three study homes in Italy with exterior wall assemblies varying between wood panel with insulation and brick construction. They obtained measured U-values of individual wall assemblies that deviated up to 31% above nominal U-values. They attributed these large deviations to the condition of wall assemblies. Estimated U-values can deviate from nominal values between 10 to 100% depending on the material type, humidity conditions, age, placement, looseness, and thickness tolerance of thermal insulation in wall assemblies [22]. Also, as-built U-values can deviate 20% above nominal U-values calculated from ISO Standard 6946 [19], [20]. Reference [11] conducted a similar study to [15] with measured U-values of individual wall assemblies that deviated up to approximately 40% above nominal U-values for heavy walls, which consisted of bricks and had higher nominal U-values than light walls, which consisted of plasterboard and several layers of thermal insulation. They attributed deviations to factors such as overall U-value and thermal mass of the entire exterior wall assembly. The heavy walls obtained more accurate results with larger overall U-values and higher thermal masses than light walls. Reference [12] measured U-values using IR thermography that deviated above nominal U-values between approximately 1% and 4% for perforated brick and thermoclay study homes in Spain. In comparison to the HFM method, IR thermography measurements of U-values are typically lower [23].

The use of IR thermography as a quantitative method can provide useful insight into the thermal comfort of a home. Human beings are considered homoiotherm organisms, meaning that constant temperatures are required at the core of the human body for the functionality of organs. The basis of thermal comfort is equilibrium between the human body and

its surrounding thermal environment. Disturbances in this equilibrium can lead to feeling hot or cold. Thermal discomfort can lead to physiological health issues such as catching a cold, hypothermia or overheating [24]. Given that air temperature is one of the six parameters affecting thermal comfort as per the American Society of Heating, Refrigerating and Air-Conditioning Engineers (ASHRAE) Standard 55 [25], thermal comfort is influenced by the heat lost from or gained in the air of a home through the exterior walls, which is affected by the amount of thermal insulation in the exterior wall assembly.

The use of IR thermography as a quantitative method can also provide useful insight into the energy consumption of a home. The amount of energy required to heat or cool a home is related to the overall U-value of the exterior wall assembly. Lower amounts of thermal insulation in a house exterior wall during the heating and cooling seasons could result in more energy being consumed for space heating and cooling, respectively. The increase in the amount of secondary energy consumed from 2012 to 2014 by single-detached houses in Canada for space heating and the relation between energy consumption and greenhouse gas emissions [26] supported the formation of initiatives such as Ontario's Climate Change Action Plan [27]. In 2015, the secondary energy use from the residential sector accounted for 17% of the total secondary energy use in Canada. The space heating and cooling secondary energy use accounted for 62% of the secondary energy use in the residential sector of Canada. The space heating and cooling secondary energy use in single detached residential houses accounted for 74% of the space heating and cooling secondary energy use in the residential sector of Canada [26]. Increases in energy demand with the forecasted 68,400 single-detached housing starts in Canada for 2018 [28] and initiatives to reduce greenhouse gas emissions require energy to be conserved in homes. Knowledge of the overall U-value of the exterior wall assemblies or areas of missing thermal insulation within exterior wall assemblies of a home can facilitate the installation of additional thermal insulation material to reduce energy consumption and related greenhouse gas emissions. Additionally, accurate estimates of overall U-values can be useful in energy modeling as they can replicate the actual performance of a building rather than providing over-estimates or under-estimates, which can incorrectly classify building energy performance and facilitate improper building retrofit decisions [14].

This study assesses the use of IR thermography as a quantitative method to estimate the overall thermal conductance value (U-value) of the exterior above-grade walls of a study home in Vaughan, Ontario.

II. Methodologies

A. Theoretical Concepts

The methodologies of this study closely followed those of [3] and [15]. The major assumption was that heat lost through exterior above-grade wall assemblies by conduction is equal to the sum of heat lost through radiation and convection on the outside surface of the brick veneer. Reference [3] used the following equation to estimate the U-value (W/m^2·K) of wall assemblies:

$$U_{MEAS} = \frac{4\varepsilon\sigma T_w^3(T_w - T_{ref}) + h_{in}(T_w - T_{in})}{T_{in} - T_{out}} \quad (2)$$

where ε is the emissivity of the wall surface building material, σ is the Stefan-Boltzmann constant (5.67x10^{-8} W/m^2·K^4), T_w is the wall surface temperature (K), T_{ref} is the wall reflective temperature (K), h_{in} is the indoor natural convection coefficient (W/m^2·K) and T_{in} and T_{out} are the indoor and outdoor air temperatures, respectively (K).

Equation (2) was modified by replacing the terms h_{in} with h_{con} and $T_w - T_{in}$ with $T_w - T_{out}$ as IR thermography measurements were conducted outdoors. The outdoor convection coefficient h_{con} was estimated using two different equations. The first equation presented by [29] assumes that convective heat loss only occurs naturally due to temperature differences between the ambient air and wall surfaces in a turbulent flow condition:

$$h_{con} = 1.31((T_s - T_f) \cdot sin\beta)^{1/3} \quad (3)$$

where T_s is the wall surface temperature (K), T_f is the air temperature (K) and β is the angle of the surface from a horizontal plane (°).

The second equation presented in the ISO Standard 6946 [19] for heat flow across an external opaque surface assumes constant natural convective heat loss plus a forced convective heat loss component as a function of outdoor wind speed:

$$h_{con} = 4 + 4v \quad (4)$$

where v is the outdoor wind speed (m/s).

The use of (2) and (3) to estimate the overall U-value is Methodology 1, whereas use of (2) and (4) to estimate the overall U-value is Methodology 2.

Reference [15] proposed a similar method under the same assumptions of heat balance. However, the radiant heat loss is estimated as the sum of the net heat lost to the surrounding air and the convective heat loss that is entirely forced from a modification of Jurges' equation that is applicable for outdoor wind speeds less than 5 m/s near the building envelope:

$$U = \frac{5.67\varepsilon_{tot}((T_i/100)^4 - (T_{out}/100)^4) + 3.8054v(T_i - T_{out})}{T_{int} - T_{out}} \quad (5)$$

where ε_{tot} is the integral emissivity of the wall surface building material, T_i is the wall surface temperature (K), T_{out} is the outdoor air temperature (K), v is the outdoor wind speed (m/s) and T_{int} is the indoor air temperature (K).

The use of (5) to estimate the overall U-value is Methodology 3.

The estimated U-values from (2) and (5) were compared to the overall U-values of the wall assembly of the study home calculated from dimensions and materials detailed in

architectural drawings and nominal values of thermal conductivity and conductance for different building materials in the wall assemblies determined from the 2009 ASHRAE Fundamentals Handbook [30]. The thermal bridging calculation for the parallel thermal resistance system between the wood studs and thermal insulation in the exterior above-grade wall assembly assumed the wood studs occupy 35% of the exterior above-grade wall area. Thermal bridging from brick ties in the exterior above-grade wall assembly was not accounted for in the calculation of the overall U-value from architectural drawings. The brick veneer and airspace were not included in the calculation of the overall U-value. To validate the overall U-value calculation from architectural drawings, the overall U-value of the study home was also calculated using utility bills. The amount of natural gas in cubic meters consumed by the home in each month during 2015 was estimated using a calendarization method. These monthly values of natural gas consumption were plotted against the number of heating degree-days below 18 °C in each month of 2015 obtained from outdoor air temperature data for Vaughan [31] to estimate the base annual natural gas consumption for domestic hot water heating. The heating degree-days were set to zero from May to August as the furnace in the study home is not in operation during these months based on homeowner preference. The plot resulted in an excellent correlation as indicated by an R^2 value of 0.98. From this plot, the base annual natural gas consumption for domestic hot water heating was assumed to be the y-intercept. To determine the total amount of natural gas consumed for only forced air heating purposes, the base natural gas consumption was subtracted from the total amount of natural gas consumed each month. These net monthly natural gas consumptions were totaled to give an estimate of the total amount of natural gas used for forced air heating in 2015. This amount of natural gas was converted to an equivalent unit of energy in kilowatt-hours using an embodied energy value for natural gas of 10.34 kWh/m^3. The foundation walls below grade could not have their surface temperatures measured through IR thermography as it was conducted entirely outdoors. Accurate thermal images of the roof could not be obtained due to the property grading and height restrictions imposed by the study home. Heat loss due to air leakage through the building envelope was not considered part of the conductive heat loss. This required heat losses from the basement, roof, and air leakage through the entire study home to be subtracted from the total amount of forced air heating energy in 2015 to estimate the exterior above-grade wall overall U-value. The basement heat losses were estimated using the ASHRAE method outlined in [29]. This method required input parameters such as the basement foundation wall perimeter, basement floor area, depth of the foundation, and average winter outdoor air temperature determined from architectural drawings of the study home and historical weather data for Vaughan [31], respectively. Another input parameter was the amplitude of the ground temperature swing, which was determined from Fig. 2.6 of [29] based on the latitudinal and longitudinal location of the study home. The conductive heat loss from the roof was estimated using the conductive heat loss equation presented by [29], annual heating degree-days, roof thermal insulation amount, and roof area. The amount of heat lost due to air leakage was determined from a calibrated HOT2000 model of the study home. The garage and cellar of the home were excluded from heat loss calculations as they are not heated. The amount of natural gas used to provide heat through forced air heating that is lost through the exterior above-grade walls of the home was approximately 21% of the total natural gas consumption. The amount of forced air heating energy lost through the exterior above-grade walls was equated to the conductive heat loss equation as a function of the U-value, exterior wall surface area, and annual heating-degree days. With the heating energy, total exterior above-grade wall surface area of the study home and number of heating degree-days for Vaughan, Ontario pre-determined, the exterior above-grade wall overall U-value was calculated to be 0.62 W/m^2·K. The nominal overall U-value of the exterior above-grade walls was calculated through an area-weighted average of the U-values of the four exterior above-grade walls of the study home calculated from dimensions and materials on architectural drawings and nominal conductivity and conductance values provided in the 2009 ASHRAE Fundamentals Handbook [30]. This value was calculated as 0.60 W/m^2·K. The overall U-value calculated from utility bills deviates 3.8% from the overall U-value calculated from architectural drawings, thus making the overall U-value from architectural drawings an appropriate nominal value in comparison to estimated overall U-values from IR thermography measurements.

B. Description of Study Home

The study home is located on 23 Nattress Street in Vaughan, Ontario. It is a two-storey, 9-meter tall single-detached home constructed in 1993. The exterior above-grade walls were built with the following materials going from the exterior to the interior according to architectural drawings: 100 mm brick cladding, 25 mm airspace, 13 mm exterior plywood sheathing, 50 mm x 150 mm wood studs 400 mm on center, RSI 3.87 fibrebatt insulation, 6 mil polyethylene vapour barrier, and 13 mm gypsum drywall sheathing. Destructive testing was not carried out to determine the as-built construction and condition of materials within the exterior above-grade walls. The building envelope includes punched double-glazed windows. The house was constructed with a stepped concrete foundation on a front split lot. The front of the house faces north with a garage incorporated into the basement. The rear yard contains dense vegetation and a downward slope of soil towards the rear of the home. The study home is equipped with a forced air heating and cooling system with a set point temperature of 20 °C annually.

C. Measurement Techniques

Exterior above-grade wall surface temperature measurements were primarily conducted using a Testo T870 thermal imager. This instrument has been calibrated under the DIN EN ISO 9001 [32] certified quality assurance system. It

contains a thermal tolerance of ±2 °C, thermal sensitivity of 100 mK, 36° x 24°/0.482 m standard lens, 320 x 240 pixel resolution (low-resolution), -15 °C to 50 °C operating temperature range, 280 °C temperature detection range, and an 8 µm to 12 µm wavelength spectral range. Surface temperatures were confirmed using a Mastercraft Digital Temperature Reader. The digital temperature reader has a -20 °C to 315 °C temperature detection range. The outdoor air temperature and relative humidity (RH) were determined using weather forecast reports and a REED R6001 thermo-hygrometer device. It contains a ±0.8 °C thermal tolerance, -20 °C to 60 °C temperature detection range, ±3% RH tolerance, and 0% to 100% RH detection range. A REED LM-8000 thermo-anemometer was used to ensure outdoor wind speeds were zero during all testing periods. It contains a ±3% wind speed tolerance, and a 0.1 to 30 m/s wind speed detection range.

Exterior above-grade wall surface temperature measurements were conducted outdoors between the hours of 11:00 P.M. to 6:00 A.M. on various days during the months of February and March in 2016 using the Testo thermal imager. The surface temperatures of the exterior above-grade walls were measured in accordance with appropriate outdoor environmental conditions to reduce the potential for erroneous results. Although the literature does not recommend measurements be taken at 11:00 P.M., a few days in February and March had overcast skies with minimal solar radiation on the brick veneer of the study home several hours prior to sunset. The in-situ emissivity of the brick cladding and double-glazed windows were determined through a calibration technique proposed by [33]. This technique uses black electrical tape with a known emissivity of 0.95 as a reference target applied to the respective surface that requires determination of its in-situ emissivity. The emissivity setting on the IR thermal imager was adjusted until the temperature of the black electrical tape was the same as the adjacent surface. The emissivity of the brick cladding and windows were determined to be 0.93 and 0.95, respectively. These emissivity values are both in line with values cited in the literature [34] [30]. Additionally, the thermal imager contained a pre-calibrated emissivity value setting for brick as 0.93.

Multiple measurements were taken on each exterior above-grade wall surface and averaged to determine the mean exterior above-grade wall and window surface temperatures. These two mean surface temperatures were then averaged using an area-weighted average to determine an average overall exterior above-grade wall surface temperature. Similarly, an area-weighted average of the emissivity values of the glass windows and brick was used to determine the mean exterior above-grade wall emissivity [35]. The reflective temperature was determined by averaging the measured surface temperatures of the foil paper placed on the exterior above-grade walls with an emissivity value of 1 as per the Reflector Method in the ASTM E1862 [36] standard. Both the electrical tape and foil paper were placed outdoors several hours prior to measurements being taken to allow for the both materials to thermally equilibrate with the outdoor climate. The individual U-values estimated for each of the four exterior above-grade walls from (2) and (5) were averaged using an area-weighted average to estimate the overall U-value of the exterior above-grade walls. A sample low-resolution thermal image generated from the study home is shown as Fig. 1.

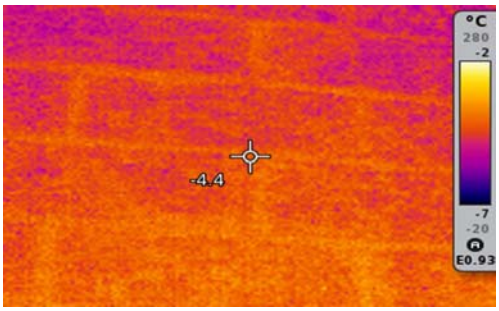

Fig. 1 Low-resolution thermal image of study home east-facing exterior above-grade wall brick veneer with airspace behind it during a testing period with an outdoor air temperature of -7°C

III. Results and Discussion

Several results of the estimated overall U-values were within ±2% to ±33% of the nominal overall U-value of the exterior above-grade walls. The remaining estimates were within -104% to +75%. The acceptable limits of deviation were assumed to be similar to those from [3] and [15]. The methodologies adapted from [3] were the most accurate for estimating the overall U-value of the exterior above-grade wall assemblies, particularly when the outdoor convection heat loss coefficient was estimated using (3). The accuracy of these methodologies suggests the need to incorporate reflective temperature of the exterior above-grade wall surfaces in determination of the overall U-value. Additionally, it suggests that it is more appropriate to estimate the convective heat loss coefficient as a function of the difference between the exterior above-grade wall surface and outdoor air temperatures. The overall U-values estimated from Methodologies 1 and 2 [3] and Methodology 3 [15] during different testing periods and their deviations from the nominal overall U-value are presented in Table I.

TABLE I
Estimated Overall U-Values ($W/m^2 \cdot K$) and Deviation (%)

Date	Time	U-value 1 (Deviation)	U-value 2 (Deviation)	U-value 3 (Deviation)
Feb 11/16	11:00 P.M.	0.82 (+36.40)	1.05 (+74.45)	0.52 (**-12.85**)
Feb 12/16	6:00 A.M.	0.78 (**+29.88**)	1.04 (+72.81)	0.62 (**+4.13**)
Feb 13/16	11:00 P.M.	0.50 (**-15.84**)	0.70 (**+16.98**)	0.46 (**-22.50**)
Feb 15/16	2:00 A.M.	0.28 (-53.74)	0.40 (**-32.93**)	0.22 (-63.91)
Feb 18/16	5:20 A.M.	0.17 (-71.98)	0.31 (-48.82)	0.30 (-50.76)
Feb 22/16	5:45 A.M.	0.51 (**-15.32**)	0.40 (**-33.18**)	-0.03 (-104.29)
Mar 03/16	5:30 A.M.	0.07 (-88.66)	0.13 (-78.26)	0.13 (-77.73)
Mar 04/16	5:30 A.M.	0.14 (-76.74)	0.26 (-56.25)	0.21 (-65.75)
Mar 04/16	11:00 P.M.	0.69 (**+14.74**)	0.79 (**+32.02**)	0.26 (-56.77)
Mar 06/16	1:00 A.M.	0.59 (**-2.32**)	0.66 (**+9.84**)	0.20 (-66.58)

The differences in estimated overall U-values between the three methodologies were significant throughout all testing

periods. This is expected given their different approaches to estimating the overall U-value. Methodologies 1 and 2 adapted from [3] incorporates the reflected surface temperature, radiant heat loss and both natural and forced convective heat losses, whereas Methodology 3 adapted from [15] incorporates the net radiant heat losses from the exterior above-grade wall surface to the surrounding outdoor air and forced convection. During all testing periods, the outdoor wind speed was zero, which removed the convective heat loss term from (5) entirely, limiting the potential for Methodology 3 adapted from [15] to be accurate in estimating overall U-values of the study home. The differences in overall U-values estimated from Methodologies 1 and 2 adapted from [3] is expected as Methodology 1 considers natural convective heat loss as a function of the difference between the exterior above-grade wall surface and outdoor air temperatures, whereas Methodology 2 considers convective heat loss as the sum of a constant for natural convection that is irrespective of exterior above-grade wall surface and outdoor air temperatures and a term that is a function of the outdoor wind speed, which was not present during the testing periods of this study, for forced convection. Methodology 1 adapted from [3] using the natural convective heat loss coefficient and Methodology 3 adapted from [15] provided mostly under-estimates of the overall U-value, while Methodology 2 adapted from [3] provided an even distribution of under and over-estimates of the overall U-value. Methodology 2 provided more over-estimates than Methodology 1 adapted from [3] and Methodology 3 adapted from [15]. This is expected as the values obtained from the equation for the convective heat loss coefficient from ISO Standard 6946 [19] are relatively high considering that they are used in the design stage of buildings to estimate heat losses [37].

Difficulty was experienced in estimating the individual U-value of the north and east exterior above-grade walls of the study home. During several early morning testing periods, the surface temperature of the brick veneer was less than the outdoor air temperature by 1 to 3 °C at the north exterior above-grade wall. This resulted in inaccurate estimates of the overall U-values with deviations from the nominal overall U-value as low as -104%. Additionally, reflective temperatures measured on the surface of the foil paper placed on the north exterior above-grade wall were extremely low in comparison to reflective temperatures measured on foil paper surfaces on the other exterior above-grade walls. Conversely, extremely large reflective temperatures were measured on foil paper surfaces during some testing periods on the east exterior above-grade wall, resulting in deviations from the nominal overall U-value as low as -89%. An IR thermography climatic parameters study by [13] mentioned that during clear sky conditions, radiation from building surfaces to the sky could cool surface temperatures. This is due to temperature differences between the sky and outdoor air surrounding buildings and the view factor of building walls with respect to the sky. The temperature differences between the sky and outdoor air allow for more heat to be lost from the building surface to the sky than is gained from the sky through radiation. The view factor with respect to the sky is the proportion of an exterior wall with unobstructed exposure to the sky. Larger view factors result in greater exterior wall surface cooling. Given the orientation of the study home, the north exterior above-grade wall has the largest sky view factor in comparison to the other exterior above-grade walls. The south exterior above-grade wall faces the rear yard, which fairly obstructs exposure to the sky due to a large number of tall trees being present. During some morning testing periods where the north exterior above-grade wall surface temperature was less than the outdoor air temperature, the cloud cover varied from 0% to 20%, suggesting clear sky radiation could have occurred. The east exterior above-grade wall views lamp pole lighting from the street that could have increased the measured reflective surface temperatures on foil paper surfaces.

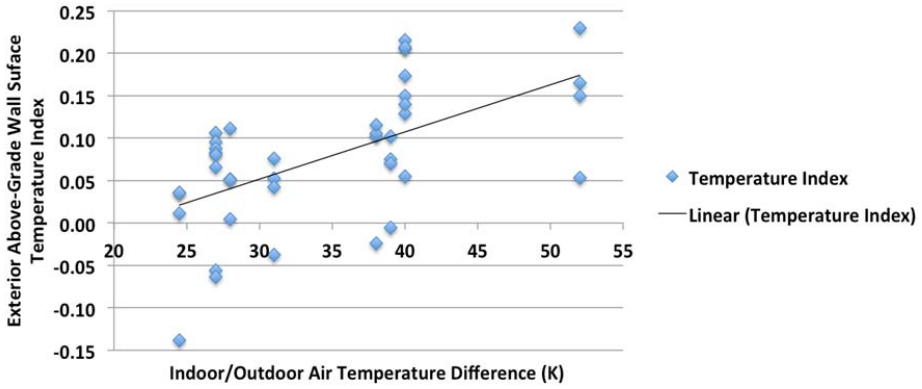

Fig. 2 Temperature index plotted against differences between indoor and outdoor air temperature during the testing periods

Larger differences between the indoor and outdoor air temperatures generally amounted to larger differences between the exterior above-grade wall surface and outdoor air temperatures. This suggests that the airspace behind the brick veneer may not be well vented and could be effectively transferring heat to the brick veneer. A temperature index, defined as the difference between the temperature of interest and the outdoor air temperature divided by the difference

between the indoor and outdoor air temperatures [39], was determined for the exterior above-grade wall surface temperatures for each testing period and plotted against the difference between the indoor and outdoor air temperature in Fig. 2. The average temperature index was 0.08, suggesting that the exterior above-grade wall surface temperatures were slightly above the outdoor air temperature.

The estimated overall U-values from all three methodologies were plotted against the difference between indoor and outdoor air temperatures in Fig. 3. In this study, the estimated overall U-values were within the ±33% accuracy limit mostly with air temperature differences less than or equal to 27 K and greater than or equal to 39 K. Given that the number of accurate estimates and their level of accuracy from an under 27 K air temperature difference is nearly the same as the number of accurate estimates and their level of accuracy from an over 39 K air temperature difference, the results indicate that greater differences in indoor and outdoor air temperature do not necessarily amount to greater accuracy of estimated overall U-values. Additionally, this suggests that the accuracy of estimated overall U-values is dependent on other factors.

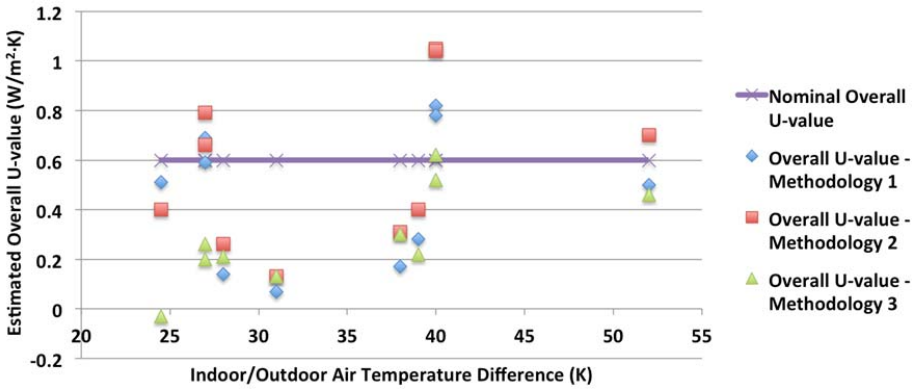

Fig. 3 Overall U-values estimated from Methodologies 1 and 2 [3] and Methodology 3 [15] plotted against the difference between indoor and outdoor air temperature during the testing periods

There are limitations to the analysis presented in this study. Measurements were conducted in less than a two-month timeframe as a result of appropriate weather conditions and access to measuring equipment. The accuracy of results could be further validated by a longer study timeframe and greater number of measurements within the testing periods. To minimize occupant disruption at extreme hours of the day, IR thermography was not conducted indoors. Estimated overall U-values from both indoor and outdoor IR thermography measurements would provide a better comparison to nominal overall U-values. The results of estimated overall U-values from indoor IR thermography measurements might obtain more accurate results given that ideal environmental conditions are present [1]. Furthermore, any effects of the airspace may be negligible as it is outboard from the interior wall surface. Utility bills and heating degree-days used to calculate the overall U-value of the exterior above-grade walls were limited to data from 2015, while measurements of surface temperatures and U-values of wall assemblies were conducted in 2016. Using the overall U-value of exterior above-grade walls obtained from utility bills and heating degree-days as validation of the calculated nominal overall U-value of exterior above-grade walls from architectural drawings, which was compared to the estimated overall U-values from IR thermography, assumes that environmental climatic conditions from 2015 and 2016 are identical, which was not the case. However, as a result of unavailable utility gas bill and heating degree-day data for 2016 given that the year had not ended during the testing period, data from 2015 were used as the most applicable substitute. The convective heat loss coefficient in (3), which produced the best results in conjunction with (2), is an equation assumed to be applicable to the study home. Reference [13] suggested that convective heat loss coefficients should be correlated to particular study homes for greater accuracy of results. The effects of temperature, relative humidity, age, and surface condition of the exterior above-grade walls on emissivity and U-value were not taken into consideration in this study. The emissivity values of the brick veneer and windows assumed ideal conditions of these building components. Age and surface-related damages can result in different emissivity values [2]. The in-situ U-values of wall assembly materials such as thermal insulation and wood studs can deviate between 5 to 50% of nominal U-values in standards as a result of the effects of age and damage [22]. Temperature and relative humidity increases are known to increase thermal conductivity of building materials [38].

IV. Sources of Error

Several sources of error were present during the testing periods. The airspace behind the brick veneer loses a portion of the heat transferred through wall assemblies due to natural convection when opposite surfaces of the airspace are at different temperatures [40]. This heat transferred could influence the temperature of the brick as natural convection circulates heat in the airspace, making the inner surface of brick warmer at higher elevations within the airspace in the presence of turbulent airflow conditions [41]. This could result

in thermal images suggesting that a large amount of heat is transferred through the exterior above-grade wall assembly and that it has a large overall U-value. Conversely, convective heat loss due to rising air could decrease the temperature of the airspace at lower elevations within the airspace [41], which would decrease the temperature of the brick, making it closer to the outdoor air temperature. This would result in thermal images suggesting that little to no heat is being transferred through the exterior above-grade wall assembly and that it has an extremely low overall U-value. Convective heat loss in airspaces of exterior wall assemblies allows for variable surface temperatures of the exterior cladding to be measured [42]. Heat transfer through airspaces is a function of several complex parameters that were unable to be determined including but not limited to airspace temperature, the Raleigh number indicating the onset of convective heat transfer as per the aspect ratio of the airspace [40], and emissivity values of the inner and outer surfaces of the airspace to determine radiant heat transfer between the inner and outer surfaces of the airspace [43], [44].

Several pieces of immovable furniture throughout the study home were against the interior surface of exterior above-grade walls, potentially impeding heat flow through particular portions of the exterior above-grade wall assemblies. Although winds were avoided during testing periods, they were potentially present a few hours prior, causing exterior above-grade wall surface temperatures to become colder due to forced convective heat losses. As previously discussed, clear sky radiation appeared to be an issue on the north exterior above-grade wall during some testing periods. During the month of March, large amounts of snow were present on the ground surrounding the study home, which potentially increased reflective temperature measurements on the surface of the foil paper placed on the exterior above-grade wall surfaces. The height of the study home resulted in the recommended maximum measurement angle of 50° to be violated occasionally in order to measure surface temperature along the height of exterior above-grade walls. The foil paper used to measure reflective temperatures was placed in a location that was accessible to the operator of the thermal imager and free of obstructions to ensure measurements of reflective temperatures could be obtained. It could not be placed in different locations along the exterior above-grade walls to validate measurements or obtain an area-weighted average. The IR thermal imager, given its thermal tolerance, fluctuated ±2 °C in surface temperature measurements at the same location on exterior above-grade wall surface. The estimated overall U-values can vary greatly as a result of a slight change in exterior above-grade wall surface temperature, as discussed in the Sensitivity Analysis section of this study. Given the close proximity to neighbouring houses on the east and west sides of the property, measured exterior above-grade wall surface temperatures on the study home could have been influenced by heat losses from the adjacent houses. The nominal overall U-value of 0.6 $W/m^2 \cdot K$ was validated with an overall U-value determined through a combination of different methods estimating heat losses through the study home, each with their own assumptions that contain sources of error. In particular, the HOT2000 model of the study home used standardized weather files [45] that were not particular to the climatic conditions that the study home was subject to during the timeframe of this study.

TABLE II
SENSITIVITY ANALYSIS RESULTS

Parameter	Varying Factor	Method 1	Method 2	Method 3
Exterior Wall Surface Temperature	±1 °C	-228% to +255%	-193% to +195%	-93% to +94%
	±2 °C	-390% to +550%	-384% to +393%	-184% to +188%
Reflective Temperature	±1°C	±183%	±95%	N/A
	±2 °C	±365%	±191%	N/A
Outdoor Air Temperature	±1 °C	-46% to +63%	-99% to +93%	-92% to 83%
	±2 °C	-47% to +156%	-205% to +180%	-192% to +162%
Indoor Air Temperature	±1 °C	±4%,	±4%	±4%
	±2 °C	-8% to+9%	-8% to +9%	-8% to +9%
Emissivity	±3%	±3%	±3%	±3%

V. SENSITIVITY ANALYSIS

A sensitivity analysis was conducted to determine which input parameters in each methodology had the greatest impact on the estimated overall U-values. As per (2) and (5), exterior above-grade wall surface temperature in degrees Kelvin is raised to the power of four, indicating that it has the greatest impact on the estimation of the overall U-value. Given the thermal tolerance of the thermal imager being ±2 °C, surface temperature measurements were varied in the sensitivity analysis accordingly. When surface temperatures of the four exterior above-grade walls were varied by ±1 °C and ±2 °C, the largest deviations in the estimated overall U-value were noted in the order of -228% to +255% and -390% to +550%, respectively. When reflective temperatures of the four exterior above-grade walls were varied by ±1 °C and ±2 °C, the largest deviations in the estimated overall U-value were noted in the order of ±183% and ±365%, respectively. Reflective temperature therefore has a lesser impact on the estimated overall U-value than exterior above-grade wall surface temperature. Other parameters such as emissivity and indoor and outdoor air temperatures demonstrated lesser impacts on the estimated overall U-value in comparison to exterior above-grade wall surface and reflective temperatures. Table II shows the results of the sensitivity analysis.

VI. FUTURE DIRECTIONS

There are certain directions that future studies should consider in order to build upon the results of this study for a

complete assessment of IR thermography estimating overall U-values of exterior above-grade wall assemblies. Firstly, testing should be conducted over longer timeframes to obtain more data prior to inferring major conclusions. Within each testing period, hourly measurements should be obtained to demonstrate the effects of overall U-value estimation over time to determine a time-averaged overall U-value, which provides greater accuracy in estimation [23]. Secondly, factors that influence the overall U-value such as temperature, relative humidity, age, and surface condition of exterior above-grade wall materials should be taken into consideration when the overall U-value calculated from architectural drawings is used as a nominal value in comparison to overall U-value estimated from IR thermography measurements. Thirdly, IR thermography measurements should be conducted both indoors and outdoors for comparative validation purposes. Fourthly, results determined from IR thermography should be compared to results from other test methods such as in the ISO Standard 9869 [17] using heat flux meters to determine the U-value of wall assemblies, which is known for determining higher U-values than IR thermography [23]. Lastly, better quality thermal imaging equipment should be used for better accuracy of measured exterior above-grade wall surface temperatures.

VII. Conclusions

IR thermography was conducted on a quantitative basis using theoretical equations from the literature to assess its feasibility in estimating the exterior above-grade wall overall U-value of a two-storey study home. Nominal overall U-values used to validate the accuracy of overall U-values estimated from IR thermography measurements were determined using architectural drawings of the study home and were verified through calendarization and weather normalization of utility bills and through other various methods of heat loss such as through a HOT2000 model of the study home. Several results of this study indicated that the overall U-values could be estimated to within ±2% to ±33% of the nominal overall U-values under ideal environmental conditions. The remaining results deviated within -104% to +75% due to uncontrollable environmental conditions such as clear sky radiation that overcooled the north exterior above-grade wall surface temperatures. The sources of error presented by outdoor environmental conditions encountered in this study necessitate the use of both indoor and outdoor IR thermography to confirm the validity of its estimated overall U-values. The accuracy of overall U-value estimation is improved with the inclusion of reflective temperature of exterior above-grade wall surfaces and convective heat loss coefficients as a function of the difference between exterior above-grade wall surface temperature and outdoor air temperature. A sensitivity analysis indicated that exterior above-grade wall surface temperature is the most influential parameter in determination of the overall U-value, which could be greatly affected by the presence of the airspace behind the brick veneer of the exterior above-grade wall assemblies, clear sky radiation, and periods of wind outdoors. Despite the lack of good quality results in every testing period during the short timeframe of this study, outdoor IR thermography may be considered a valid non-destructive test method in estimating the overall U-value of low-rise residential homes under ideal environmental testing conditions and in comparison with additional test methods to validate results.

Acknowledgment

M. D. Baffa thanks Mr. Nick Tassone, President of Building Sciences Inc., for providing infrared thermography and other required equipment to facilitate this study.

References

[1] D. J. Titman, "Applications of thermography in non-destructive testing of structures," *NDT & E International*, vol. 34, no. 2, pp. 149–154, Mar. 2001.

[2] N. P. Avdelidis, and A. Moropoulou, "Emissivity considerations in building thermography," *Energy and Buildings*, vol. 35, no. 7, pp. 663–667, Aug. 2003.

[3] P. A. Fokaides, and S. A. Kalogirou, "Application of infrared thermography for the determination of the overall heat transfer coefficient (U-Value) in building envelopes," *Applied Energy*, vol. 88, no. 12, pp. 4358–4365, Dec. 2011.

[4] C. A. Balaras, and A. A. Argiriou, "Infrared thermography for building diagnostics," *Energy and Buildings*, vol. 34, no. 2, pp. 171-183, Feb. 2002.

[5] A. Moropoulou, M. Koui, N. P. Avdelidis, E. T. Delegou, and S. Kouris, "Calculating the emissivity of building materials for infrared thermographic applications," in *Proceedings of the 6th International Conference of the Slovenian Society of NDT*, 2001, pp. 333–337.

[6] R. A. Thomas, *The thermography monitoring handbook*. Oxford: Coxmoor Publishing, 1999.

[7] A. Kylili, P. A. Fokaides, P. Christou, and S. A. Kalogirou, "Infrared thermography (IRT) applications for building diagnostics: A review," *Applied Energy*, vol. 134, pp. 531–549, Dec. 2014.

[8] S. Datcu, L. Ibos, Y. Candau, and S. Matteï, "Improvement of building wall surface temperature measurements by infrared thermography," *Infrared Physics & Technology*, vol. 46, no. 6, pp. 451–467, Aug. 2005.

[9] E. Barreira, and V. P. de Freitas, "Evaluation of building materials using infrared thermography," *Construction and Building Materials*, vol. 21, no. 1, pp. 218–224, Jan. 2007.

[10] J. M. Hart, *A practical guide to infra-red thermography for building surveys*. Watford: Building Research Establishment, 1991.

[11] R. Albatici, A. M. Tonelli, and M. Chiogna, "A comprehensive experimental approach for the validation of quantitative infrared thermography in the evaluation of building thermal transmittance," *Applied Energy*, vol. 141, pp. 218–228, Mar. 2015.

[12] B. Tejedor, M. Casals, M. Gangolells, and X. Roca, "Quantitative internal infrared thermography for determining in-situ thermal behaviour of façades," *Energy and Buildings*, vol. 151, pp. 187–197, Jun. 2017.

[13] B. Lehmann, K. Ghazi Wakili, T. Frank, B. Vera Collado, and C. Tanner, "Effects of individual climatic parameters on the infrared thermography of buildings," *Applied Energy*, vol. 110, pp. 29-43, Oct. 2013.

[14] A. Marshall, J. Francou, R. Fitton, W. Swan, J. Owen, and M. Benjaber, "Variations in the U-Value Measurement of a Whole Dwelling Using Infrared Thermography under Controlled Conditions," *Buildings*, vol. 8, no. 3, pp. 46, Mar. 2018.

[15] R. Albatici, and A. M. Tonelli, "Infrared thermovision technique for the assessment of thermal transmittance value of opaque building elements on site," *Energy and Buildings*, vol. 42, no. 11, pp. 2177–2183, Nov. 2010.

[16] E. Grinzato, V. Vavilov, and T. Kauppinen, "Quantitative infrared thermography in buildings," *Energy and Buildings*, vol. 29, no. 1, pp. 1–9, Dec. 1998.

[17] ISO 9869 Thermal insulation - Building elements - In-Situ Measurement of Thermal Resistance and Thermal Transmittance. Part 1: Heat Flow Meter Method, 2014.

[18] M. O'Grady, A. A. Lechowska, and A. M. Harte, "Infrared

thermography technique as an in-situ method of assessing heat loss through thermal bridging," *Energy and Buildings*, vol. 135, pp. 20–32, Nov. 2016.
[19] EN ISO 6946 Building components and building elements – thermal resistance and thermal transmittance – Calculation method, 2007.
[20] S. Doran, *Field investigations of the thermal performance of construction elements as built. BRE Client Report No. 78132. A DETR Framework Project Report.* East Kilbride: Building Research Establishment (BRE), 2001.
[21] L. Evangelisti, C. Guattari, P. Gori, and R. D. L. Vollaro, "In situ thermal transmittance measurements for investigating differences between wall models and actual building performance," *Sustainability*, vol. 7, no. 8, pp. 10388–10398, Aug. 2015.
[22] UNI 10351 Building Materials. Thermal Conductivities and Vapor Permeabilities, 1994.
[23] E. Lucchi, "Applications of the infrared thermography in the energy audit of buildings: A review," *Renewable and Sustainable Energy Reviews*, vol. 82, no. 3, pp. 3077–3090, Feb. 2018.
[24] M. V. Jokl, "Thermal comfort and optimum humidity Part 1," *Acta Polytechnica*, vol. 42, no. 1, 2002.
[25] ASHRAE Standard 55 Thermal Environmental Conditions for Human Occupancy, 2017.
[26] Statistics Canada, *Report on Energy Supply and Demand in Canada 1990–2015*. Ottawa: Statistics Canada, 2017
[27] Government of Ontario, *Ontario's Five Year Climate Change Action Plan 2016 - 2020*. Government of Ontario, 2016.
[28] Canadian Mortgage and Housing Corporation, *Housing Market Outlook - Canada Edition*. Canadian Mortgage and Housing Corporation, 2017.
[29] T. A. Reddy, J. F. Kreider, P. S. Curtiss, and A. Rabl, *Heating and Cooling of Buildings: Design for Efficiency, Revised Second Edition*. Boca Raton: CRC Press, 2009.
[30] ASHRAE, *2009 ASHRAE Handbook - Fundamentals* (Har/Cdr edition). Atlanta: ASHRAE, 2009.
[31] Environment Canada. 2016. Temperature – Monthly data for Vaughan. Retrieved March 11, 2016, from https://vaughan.weatherstats.ca/charts/temperature-monthly.html.
[32] DIN EN ISO 9001. Quality management systems — Requirements, 2008.
[33] R. P. Madding, "Emissivity measurement and temperature correction accuracy considerations," in *Thermosense XXI*, Orlando, 1999, pp. 393-402.
[34] R. Albatici, F. Passerini, A. M. Tonelli, and S. Gialanella, "Assessment of the thermal emissivity value of building materials using an infrared thermovision technique emissometer," *Energy and Buildings*, vol. 66, pp. 33–40, Nov. 2013.
[35] R. -H. Zhang, et al., "Study of emissivity scaling and relativity of homogeneity of surface temperature," *International Journal of Remote Sensing*, vol. 25, no. 1, pp. 245–259, Jan. 2004.
[36] ASTM E1862 Standard test methods for measuring and compensating for reflected temperature using infrared imaging radiometers, 2002.
[37] G. Dall'O, L. Sarto, and A. Panza, "Infrared screening of residential buildings for energy audit purposes: results of a field test," *Energies*, vol. 6, no. 8, pp. 3859–3878, Jul. 2013.
[38] I. Valovirta, and J. Vinha, "Water vapor permeability and thermal conductivity as a function of temperature and relative humidity," *Performance of exterior envelopes of whole buildings IX*, 2004.
[39] N. B. Hutcheon, and G. O. P. Handegord, *Building science for a cold climate (First Edition)*. Toronto: John Wiley & Sons, 1984.
[40] S. Lorente, "Heat losses through building walls with closed, open and deformable cavities," *International Journal of Energy Research*, vol. 26, no. 7, pp. 611–632, Jun. 2002.
[41] J. Xamán, G. Álvarez, L. Lira, and C. Estrada, "Numerical study of heat transfer by laminar and turbulent natural convection in tall cavities of façade elements," *Energy and Buildings*, vol. 37, no. 7, pp. 787–794, Jul. 2005.
[42] A. Colantonio, "Identification of convective heat loss on exterior cavity wall assemblies," in *Thermosense XXI*, Orlando, 1999, pp. 514–520.
[43] B. Kersten, and J. van Schijndel, "Modeling the Heat Exchange in Cavities of Building Constructions Using COMSOL Multiphysics®", n.d.
[44] S. -Y. Wu, L. Xiao, Y. Cao, and Y.-R. Li, "Convection heat loss from cavity receiver in parabolic dish solar thermal power system: A review," *Solar Energy*, vol. 84, no. 8, pp. 1342–1355, Aug. 2010.
[45] D. Haltrect, and K. Fraser, "Validation of HOT2000^{TM} Using HERS BESTEST", in *Proc. Building Simulation*, Prague, 1997, pp. 1-8.

Matthew D. Baffa completed the Bachelor of Applied Science (BASc) Civil Engineering program in 2015 and the Master of Engineering (MEng) Civil Engineering program in 2016 both at the University of Toronto in Toronto, Ontario. His major field of study is in the Building Science specialization of Civil Engineering. He is now a Project Manager and Engineering Intern (EIT) at Building Sciences Inc. in Concord, Ontario.